Design and Development of an Advanced Real-Time Satellite Simulator

Ja-Young Kang, Jae-Moung Kim, and Seon Jong Chung

CONTENTS

ABSTRACT

An advanced real-time satellite simulator (*ARTSS*) has been developed to support the ground operations activities of the ETRI satellite control system, such as testing of the system facilities, validation of flight control procedures, verification of satellite commands as well as training of the ground operators. The design of *ARTSS* is based on the top-down approach and makes use of a modular programming to ensure flexibility in modification and expansion of the system. Graphics-based monitoring and control facilities enhance the satellite simulation environment. The software spacecraft model in *ARTSS* simulates the characteristics of a geostationary communication satellite using a momentum bias three-axis stabilization control technique. The system can be also interfaced with a hardware payload subsystem such as Ku-band communication transponder to enhance the simulator capability. Therefore, *ARTSS* is a high fidelity satellite simulation tool that can be used on low-cost desk top computers. In this paper, we describe the design features, the simulation models and the real-time operating functions of the simulator.

I. INTRODUCTION

Most satellite simulators can be divided into three groups according to their usage; development, integration and verification, and operations. A subsystem simulator, such as a solar array simulator or a battery simulator, is a typical development simulator. This kind of simulator is used to analyze the characteristics of the subsystem or to evaluate the design parameters. Integration and verification simulators are used for hardware-hardware or hardware-software interface validation and integration and test procedures validation. Satellite operations simulators are used for ground systems checkout, command and telemetry validation, and satellite operation team training. Satellite operations simulators may be divided further into static and dynamic simulators [1]. The former is designed to process stored events and the latter, for a simulator that models the spacecraft's dynamics as realistically as possible. Some dynamic simulators include hardware in the simulator loop [2]. Hardwares included may be onboard computer, sensors, or actuators.

Nowadays, desktop computers are capable of performing millions of instructions per second and give us the computing power needed to execute complex mathematical models in the real-time. The software models running on such computing devices can simulate the functions of most hardware subsystems with relatively high precision. A simulator using software models has more flexibility in developing simulation models and requires less expense than one involving hardware.

An advanced real-time satellite simulator (*ARTSS*) is a workstation-based, real-time satellite simulation system. It uses a software spacecraft model consisting of both the static and dynamic models and the hardware transponder. It provides many graphic monitoring and control facilities and supports both pre-operational and operational phases of a communication satellite system. *ARTSS* will be used primarily for the testing and validation of ground operation control center facilities and flight-control procedures and strategies, as well as for training satellite operations personnel in both satellite and ground segment procedures.

II. SYSTEM CONFIGURATION AND DESIGN CONCEPT

ARTSS is designed to run in the operational environment shown in Fig. 1. The main computer is a DEC VAXstation 4000/60 with 32 MB main memory and 1GB hard disk drive, using the VMS operating system. Two IBM PCs are used to provide graphic visualization of three-dimensional attitude and orbital motion of the satellite. A terminal server is used to provide RS232C serial communication link to the TTC system and transponder. The computers and terminal server are connected by LAN. The programming language is VAX C and FIGES and MOTIF/XLib are used to support the GUI facilities.

To increase the system maintainability,

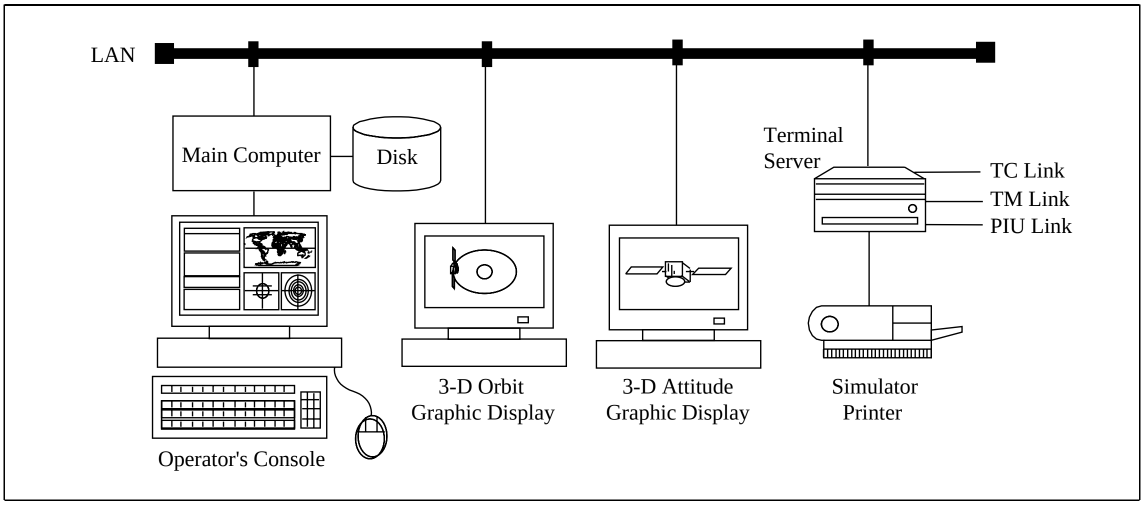

Fig. 1. *ARTSS* system configuration.

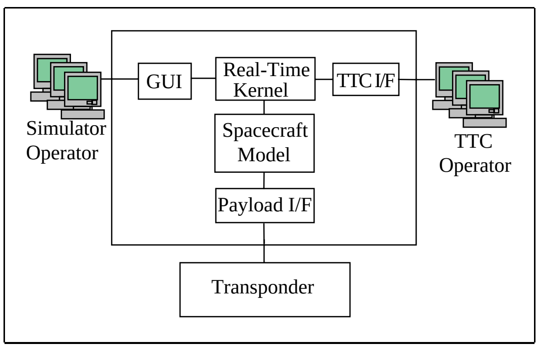

Fig. 2. Functional block diagram.

a top-down design approach and a modular programming concept were used. The software consists of three functional blocks; the real-time kernel block, the satellite model block, and the interface block (Fig.2). The real-time kernel block consists of a telecommand handling unit (TCMHU), a telemetry handling unit (TLMHU), a command execution unit (CMDEU), a graphic user interface handling unit (GUIHU), a telemetry display unit (TLMDU), a graphic display unit (GRPDU), and a shared memory section. The satellite model block consists of an attitude and orbit control subsystem unit (AOCSU), an electric power subsystem unit (EPSU), a thermal control subsystem unit (THCSU), a telemetry command and ranging subsystem unit (TCRSU), and a payload subsystem unit (PLDSU). The interface block is composed of a graphic interface unit (GUI), a TTC interface unit (TTCIU), and a transponder interface unit (XPDIU). The interprocess communication means among the units are mailboxes and shared memory provided on VAX/VMS. Figure 3 shows the internal data flows between the software units.

III. REAL-TIME KERNEL

A prime requirement is that the simula-

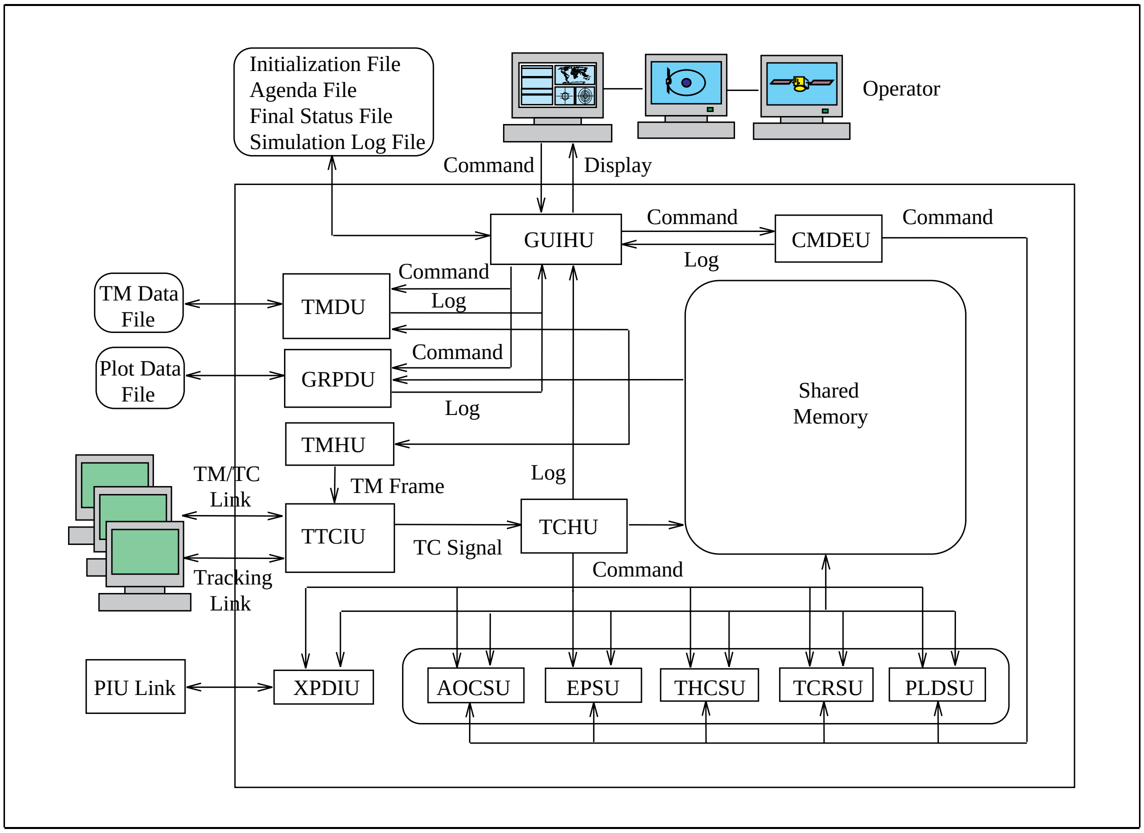

Fig. 3. System software structure.

tor run efficiently in real-time with the corresponding satellite control center (SCC) software. In other words, the simulator should generate accurate digital telemetry data in response to appropriate satellite control commands and provide the telemetry and monitoring data at realistic intervals and rates sufficiently close to real-time.

The real-time kernel has four control functions consisting of simulator command processing, telemetry processing, model scheduling and control, and simulation data recording and display. The command processing function consists of receiving, decoding, validating and executing satellite commands sent to the simulator via GUI or TTC interface. The telemetry processing function controls the format and content of the simulated telemetry data, and sends them to the outside. In the normal mode, *ARTSS* generates and transmits a telemetry frame of 256 words every two seconds. Since one major frame is composed of 25 minor frames, it takes about 50 seconds for complete transmission. In the dwell mode, the maximum period for generation and transmission of the telemetry is 0.25 seconds. In the normal mode, the individual subsystem process runs with a primary period of 0.25 seconds. For the attitude dynamics module, the period is 0.01 seconds and for the electric power subsystem unit, it is 2 seconds. Under peak loading conditions, the CPU load does not exceed 70 percent of the CPU allocation for the program that should be executed in real-time on the host computer.

IV. SATELLITE SIMULATION MODELS

The model satellite used for *ARTSS* is a typical geosynchronous communication satellite with a momentum bias three-axis-stabilization control system [3]. The advantages of the momentum bias control system are (1) roll-yaw coupling that permits yaw angle stabilization without a yaw sensor for pitch axis pointing, and (2) a momentum wheel that may be used as an actuator for pitch angle control and that provides scanning motion across the celestial sphere for a horizon sensor. Thus, momentum bias systems can provide three-axis control with less instrumentation than a three-axis reaction wheel system. The satellite model block contains the satellite subsystems and environment models. This comprises an attitude and orbit control subsystem (AOCS) model, an electric power subsystem (EPS) model, a telemetry, command and ranging subsystem (TCRS) model, a thermal control subsystem (THCS) model and a payload subsystem (PLDS) model as shown in Fig. 4. The prime requirement for the simulation models is that modeling be sufficiently detailed to generate telemetry data that is realistic when compared to that of the in-orbit satellite. The models periodically output telemetry data, which are stored in the shared memory as raw values and forwarded to the telemetry handling unit for formating. The models accept satellite commands on their mailboxes and change their states to appropriate forms.

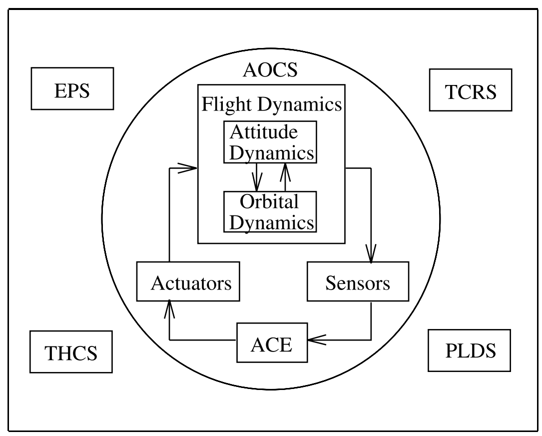

Fig. 4. Satellite model block diagram.

1. AOCS

The AOCS unit supports two sequential mission phases. The first phase is related to the pre-operational mission period, which is from the time of the satellite's injection from its launch vehicle into the transfer orbit, throughout the transfer orbit, and to the initiation of the earth acquisition in the geosynchronous orbit. The second phase is related to the operational mission period, which is from the onset of the initial earth acquisition to the end of the mission lifetime of the satellite. In an actual satellite system, the AOCS consists of the sensors, actuators and control electronics needed to maintain and monitor the satellite pointing requirements and control the required maneuvers during the period of all phases of satellite mission life. In *ARTSS*, the satellite flight dynamics models are included in the AOCS.

In the preoperational phase, the AOCS uses redundant sun sensors, horizon sensors, thrusters, and component selection and thruster firing logic and circuitry. The spacecraft, spinning at approximately 50 rpm about its maximum moment of inertia axis, is injected into the transfer orbit. A series of maneuvers controlled by thrusters accomplishes spin-axis precession, properly orienting the apogee kick motor thrust axis, and spin rate adjustment to 60 rpm. Injection into geosynchronous orbit is achieved no earlier than on the required apogee pass, after which the spacecraft spin rate is reduced to 5 rpm. A further reorientation aligns the spin axis with the positive orbit normal. The body axes are then rotated with respect to the inertial fixed angular momentum vector via a dual-spin turn so that the momentum wheel axis(spacecraft pitch axis) aligns with the positive orbit normal. The spin rate is then reduced to allow solar panel deployment and pitch capture.

In the operational phase, the AOCS uses a three-axis attitute control technique. A pitch momentum wheel assembly (MWA) facilitates full three-axis control by virtue of the gyroscopic stiffness of the wheel axis in inertial space and its servo-controlled exchange of angular momentum with the spacecraft main body. A pivot mechanism is used to reorient the MWA momentum vector in the spacecraft pitch-yaw plane by tilting the MWA about roll axis. Roll and pitch attitude are determined by an earth sensor assembly (ESA). Continuous control of the pitch-axis alignment to the orbit normal is accomplished by magnetic torquing.

A. Flight Dynamics Model

The flight dynamics model (FDM) consists of the orbital and attitude dynamics. The orbital dynamics model includes the natural perturbations due to the sun and moon's attraction, the solar wind and the effect of the mass distribution of the earth. The satellite is modeled as a two-body system consisting of an asymmetric rigid-body, representing the spacecraft, and a rotating wheel, representing the momentum wheel assembly. The attitude dynamics model includes dynamic equations, kinematics equations, and electrical torque equations.

In the operational phase, roll and pitch angles are measured in reference to the satellite geocentric vector and are computed from the current attitude information. Disturbance torque model indicated by the apogee kick motor (AKM) thrust misalignment is included. The FDM evolves the satellite geocenter vector, but does not model the satellite's orientation with respect to any body other than the earth.

The FDM inputs torque from the roll/yaw torquer (RYT), pivot angle, and thruster torques and forces. It calculates the combined torques acting on the satellite, modifies the state of the model based on the combined forces, and updates the satellite orbit. The torque for each thruster is obtained from the torque-force table. The total torque is evaluated by summing torques from all thrusters presently firing and passed to the FDM. The orbit dynamics model is as follows:

$$\ddot{\underline{r}}+\frac{\mu}{r^3}\underline{r}=\underline{a}_{AKM}+\underline{a}_{Thrust}+\underline{a}_{SRP}+\underline{a}_{Sun}+\underline{a}_{Moon}+\underline{a}_{Earth}, \quad (1)$$

where

$\underline{r}$ = position vector from the earth center to the center of mass of the spacecraft,

μ = gravitational parameter,

$\underline{a}_{AKM}$ = acceleration vector due to apogee kick motor firing,

$\underline{a}_{Thruster}$ = acceleration vector due to combined propulsion system operation,

$\underline{a}_{SRP}$ = acceleration vector due to solar radiation pressure,

$\underline{a}_{Sun}$ = acceleration vector due to sun attraction,

$\underline{a}_{Moon}$ = acceleration vector due to moon attraction, and

$\underline{a}_{Earth}$ = acceleration vector due to effect of uneven earth mass distribution.

In geosynchronous orbit, the aerodynamic acceleration term can be dropped because it is small when compared with other terms.

The attitude dynamics model is as follows:

$$\dot{\underline{H}}=-\tilde{\underline{\omega}}\underline{H}+\underline{T}_{Thruster}+\underline{T}_{RYT}+\underline{T}_{Disturbance}, \quad (2)$$

$$\dot{\underline{H}}_{Wheel}=-(\tilde{\underline{\omega}}_{Body}+\tilde{\underline{\omega}}_{Wheel})\underline{H}_{Wheel}+\underline{T}_{Wheel}, \quad (3)$$

$$\dot{q}=\frac{1}{2}\begin{bmatrix}-\tilde{\underline{\omega}} & \underline{\omega}\\ -\underline{\omega}^T & 0\end{bmatrix}\underline{q}, \quad (4)$$

where

$$\underline{H}=\underline{H}_{Body}+\underline{H}_{Wheel}$$
$$=\underline{\underline{I}}_{Body}\underline{\omega}_{Body}+\underline{\underline{I}}_{Wheel}(\underline{\omega}_{Body}+\underline{\omega}_{Wheel})-M_{Body}\tilde{\underline{r}}_B\tilde{\underline{r}}_B\underline{\omega}_{Body}-M_{Wheel}\tilde{\underline{r}}_W\tilde{\underline{r}}_W\underline{\omega}_{Body}$$

= total angular momentum of the system,

$\underline{\underline{I}}_{Body}$ = inertia matrix of the spacecraft body,

$\underline{\underline{I}}_{Wheel}$ = inertia matrix of the wheel,

M_{Body} = mass of the spacecraft body,

M_{Wheel} = mass of the wheel,

$\underline{\omega}_{Body}=(\omega_{B_x}\ \omega_{B_y}\ \omega_{B_z})^T$

= spacecraft body angular rate vector,

$\underline{\omega}_{Wheel}=(\omega_{W_x}\ \omega_{W_y}\ \omega_{W_z})^T$

= wheel angular rate vector relative to the body,

$\underline{r}_B$ = position vector from the center of mass of the system to the center of mass of the body,

$\underline{r}_W$ = position vector from the center of mass of the system to the center of mass of the wheel,

$\underline{q}=(q_0\ \ q_1\ \ q_2\ \ q_3)^T$ = Euler parameters,

$\underline{T}_{Thruster}$ = torque vector due to combined propulsion system thrusting,

$\underline{T}_{RYT}$ = roll and yaw torque vector due to magnetic torquer,

$\underline{T}_{Disturbance}$ = torque vector due to AKM misalignment and solar radiation pressure,

$\underline{T}_{Wheel}$ = momentum wheel torque vector,

and $(\tilde{\ })$ = skew symmetric matrix formed from the indicated 3×1 matrix, e.g., $\underline{\omega}$.

The gravity gradient and aerodynamic torques are not included in (2) because they are small in high altitude orbit such as a geosynchronous orbit. If the pivot is set in a certain position for attitude trim of the roll-axis, the spin axis of the wheel is fixed in the body and the attitude variables can be reduced to

$$\underline{x} = \left(\omega_{B_x}\ \ \omega_{B_y}\ \ \omega_{B_z}\ \ \omega_{W_s}\ \ q_0\ \ q_1\ \ q_2\ \ q_3\right)^T, \qquad (5)$$

where ω_{W_s} is the angular rate of the wheel about its spin axis.

B. Sensor Models

The sensor models process ephemeris data from the FDM and produce telemetry and attitude information for the attitude control electronics model (ACEM). The sensor models consist of the horizontal sensor assembly model (HSAM), the sun sensor assembly model (SSAM), the earth sensor assembly model (ESAM) and the rate measuring assembly model (RMAM).

The HSAM consists of two functionally independent bolometer telescope assemblies containing thermistor bolometer detectors with optics and processing electronic circuitry in an integral assembly and being rotated about the spin axis by 45 degrees with respect to each other. The HSAM is used to determine time lags between the command eye pulses generated by the SSA and the earth crossing envelops produced by two bolometer telescope assemblies of the HSA.

The SSAM consists of redundant detector assemblies and associated electronics used to determine the sun angle with respect to the spin axis of satellite while it is on the transfer orbit and the phasing of a satellite reference axis with respect to the sun.

The ESAM determines roll and pitch errors of the satellite with respect to the earth center during the period of operational mission phase which is most of satellite's life time. It measures roll and pitch attitude by scanning the fields of view of two pencil-beam bolometers across the earth in an east-west direction and looking for the difference in radiation between the earth and space in the 14 to 16 microns band. Pitch and roll outputs from the ESAM include Gaussian noise.

During north/south (N/S) stationkeeping maneuvers, auxiliary active control is used to maintain pointing accuracy. Since N/S maneuvers produce high disturbances primarily about the roll and yaw axes, rate measuring assemblies (RMAs) are oriented along each of these axes to provide high-bandwidth measurements of attitude error. The RMAs contain single-axis rate integrating gyros which provide to the attitude control electronics (ACE) digitized roll and yaw angle increment signals. The filtered and bias-corrected signal is integrated into a yaw or roll angle estimate available for the control logic. In order to determine the bias value needed to correct for gyro drift, the RMA is turned on at least 60 minutes prior to a planned maneuver and the drift rate is allowed to stabilize. Just prior to the maneuver start, the integrated roll and yaw estimates are initialized and the bias value is calculated by the ACE in the following manner. The average RMA drift rate is calculated for two 8-second sampling periods, with the initiation of each sampling period seperated by one-half the satellite nutation period. The bias value is the average of these two average drift rates. It shoud be noted that this initialization procedure will interpret any actual roll and yaw attitude rates present on the spcecraft as biases in the respective RMA. The initialization process for each RMA is different. The roll error signal from the ESA is used to initialize the roll RMA. At the time of initialization, the current value of the 8-second average of the processed ESA roll-error signal is used as the current estimate of the satellite roll error. In the absence of any relative yaw error measurement, the yaw RMA is initialized to zero. Values for the pitch error during N/S maneuvers are provided by the ESA. To minimize the effects of any variation in gyro drift after initialization, the roll gyro drift rates and gyro roll angle are continuously updated from the ESA 8-second average at time intervals that are selectable by ground command. Intervals of 64, 128, 256, and 8192 seconds are available. The nominal value is 256 seconds, which is the default when the ACE is first switched on. Yaw gyro output is not updated similarly because no yaw reference is available.

C. ACEM

The ACEM simulates all the attitude control subsystem functions of the satellite attitude control electronics during the preoperational and operational phases. The phases correspond to the transfer and geosynchronous orbits, respectively.

The ACEM accepts satellite commands, sensor data, and anomaly requests as input, modifies and updates its operating state accordingly, and produces telemetry and actuator commands as output. The satellite commands are routed by the command execution unit. The sensor data are angle and rate information produced by the HSAM, SSAM, ESAM and RMAM. The anomaly settings are generated by the operator at the ACEM menu. Actuator commands are output to the roll yaw torquer model (RYTM), the momentum wheel assembly model (MWAM) and the thrusters. In the operational mode, roll and pitch angles are input from the ESAM and roll and yaw angles are input from the RMAM.

D. Actuators Models

The actuator models consist of the RYTM, MWAM, combined propulsion system model (CPSM), and AKMM. Actuator models produce forces and torques corresponding to commands from the ACEM and ground control center and output them to the FDM.

The RYTM provides a magnetic dipole moment such that its interaction with the earth's magnetic field creates control torques. When energized, the RYTM provides a magnetic dipole moment. The polarity of the dipole moment depends on the polarity of the applied voltage. The torque on the spacecraft generated by the RYT depends on the polarity of the dipole moment and on the orientation of the RYT with respect to the earth's magnetic field. The RYT has a constant torque capacity. The output of the RYTM consists of telemetry and torques sent to the FDM. The mathematical expression for the magnetic torque is as follows:

$$\underline{T}_{RYT} = \underline{M} \times \underline{B}, \tag{6}$$

where

$\underline{M} =$ dipole moment vector

and $\underline{B} =$ earth magnetic field vector.

In the MWAM, there are two MWAs on the satellite, each attached to its own pivot assembly. The pivot positions the spin axis (momentum vector) of the MWA for on-orbit attitude trim of the roll axis. The pivot itself was modeled as a massless rod and the attitude trimming is assumed static. Motion of the pivot is electrically limited to ± 2.3 degrees, and a means is provided of driving the pivot to its zero position by ground command. The MWA provides angular momentum storage and reaction torque capability about the spin axis of the MWA rotor. The MWAM contains an inertia wheel which is driven by a motor to a speed which is commandable from the ground or from the ACEM. The MWAM includes the wheel speed feedback necessary to achieve the demanded speed. The MWAM outputs speed demands to the MWA dynamics model in the FDM. The effective wheel torque is the difference between the nominal output torque and the total friction torque :

$$\underline{T}_{Wheel} = \underline{T}_{Nominal} - \underline{T}_{Viscous} - \underline{T}_{Coulomb}\,. \tag{7}$$

When no saturation is present, the spin axis component of the efficient wheel torque is

$$T_{Wheel} = \frac{K_T}{Z + AG}(GV_A - K_B\omega) - F_V\omega - T_{Coulomb}\,, \tag{8}$$

$$V_A = K_A(K_C V_C + V_{Bias} - K_F\omega), \tag{9}$$

$$Z = \frac{R}{1 + \frac{24\omega\tau}{\pi}\exp\left(-\frac{\pi}{24\omega\tau} - 1\right)}, \tag{10}$$

where

A = current feedback gain constant,
G = forward voltage gain of power amplifier,
K_A = summing amplifier gain,
K_B = motor back EMF constant,
K_C = speed demand weighting factor,
K_F = tach feedback gain,
K_T = motor torque constant,
R = total resistance of motor circuit from motor bus terminal to power ground,
V_A = torque-speed demand voltage limits,
V_{Bias} = bias voltage,
V_C = command voltage,
ω = wheel speed in normal mode, and
τ = motor inductive time constant.

The CPSM consists of the rocket engine assembly model (REAM) and the electrothermal hydrazine thruster model (EHTM). They provide forces and torques to the FDM according to commands from the ACEM and the

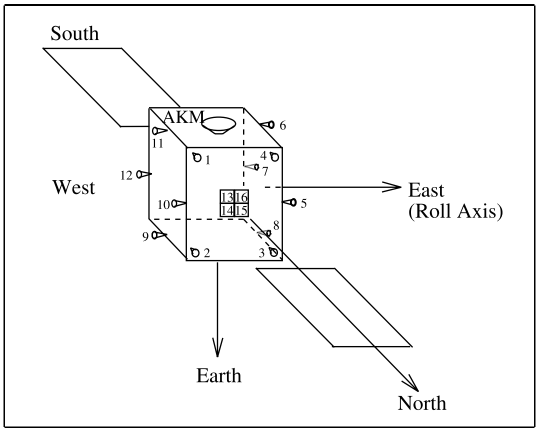

Fig. 5. Thruster locations.

ground control center. Forces and torques produced by each thruster, REAs and EHTs, are stored in the torque-force table. In the REAM, the REAs are used in either a pulse mode and/or steady-state (continuous firing) mode, depending on the demand. The total torque on the satellite resulting from the REA firing is calculated. The REA torque variation due to the tank pressure variation is not modeled. An eleven-second timer is set when thruster firing is manually commanded or "start timer" is commanded. All ground commanded REA firings are terminated if the eleven-second timer expires prior to being reset. The eleven-second timer has no effect on REA firing commanded by the ACE. Failure of eleven-second timer is modeled such that if the timer is failed, manual thruster firing is not terminated when the timer fails to expire. The outputs of the REAM function consist of telemetry and torque data sent to the FDM. In the EHTM, four EHTs (thruster 13, 14, 15, and 16) are used in steady-state mode for the primary N/S stationkeeping maneuvers. The EHTs can be fired only in either odd (13/15) or even (14/16) pairs (Fig.5). It is necessary to enable the appropriate pairs of EHTs prior to initiating firing of these thrusters. The enable/disable thruster command is executed via an EHT control assembly model (ECAM).

2. EPS

The primary function of the EPS is to provide the unregulated power required to operate the satellite for its lifetime in orbit. The EPSM simulates functions of the solar array, solar array drive, battery, charge regulator, power supply electronics, and battery pull-up assembly. In the preoperational mission phase, the solar array is stowed and partially operational. In the operational mission phase, i.e., geosynchronous orbit, the EPS has four operating modes. When the satellite is in an eclipse, the EPS discharges the battery to supply the required power and it recharges the battery with the power generated by the solar array during daytime. The EPS keeps trickle-charge for maintaining the battery in full charge except for the EHT firing mode. The battery repeats deep-discharge and pull-up for reconditioning to prepare for the eclipse season. The peak time in the power consumption occurs at the EHT firing mode. During this time, the battery is disconnected from the solar array and supplies the power to the EHT. Only the solar array supplies power to the unregulated bus. During the EHT operation, it is necessary to prevent power fluctuation. The model outputs telemetry data to the shared memory.

3. THCS

The THCS model simulates the switching status of the heaters and calculates the node temperatures on the satellite in accordance with the sun angles. The model outputs telemetry data to the shared memory. Most of thermal commands are in the category of enabling/disabling heaters and heater control units.

4. TCRS

The TCRS is modeled to simulate only the switching status of the TC&R subsystem of the satellite. Telecommand and telemetry processing functions are included in the simulator kernel block.

5. PLDS

The key feature of the payload subsystem model is a capability of interfacing the real Ku-band transponder to *ARTSS*. In this case, the model collects telemetry data directly from the hardware transponder and passes them to the shared memory.

V. OPERATING FACILITIES

1. Graphic User Interface

The graphic user interface (GUI) of *ARTSS* provides monitoring and control facilities for the simulator by acting as a layer between the user and the kernel of the simulator, to which it is coupled via service calls. Based on the OSF/Motif windows standard, it supports the simulator control and the satellite commanding as well as the simulation monitoring by means of alphanumeric representations, trend graphs and three-dimensional graphic animation in real time. This block includes the GUI handling unit, the graphic display unit and the telemetry display unit. The user interfaces with *ARTSS*, directly via VAX station 4000/60. The operator is provided with the password necessary to login to the station and to start the simulator. In the main console, the following windows are provided (Fig. 6):

A. Commander Window

A simulator control command is entered on a command line by the operator. The facility checks the validity of the command syntax before actually sending the input command to the simulator kernel. Functions accessible from the user include initialization, startup and shutdown, pause and continue, simulation speed control, telemetry display and monitoring, telemetry modification, event file processing, and anomaly introduction.

B. Telemetry Display

This function visualizes telemetry variables, arranged in tables, in alphanumeric format. The operator can define the layout and se-

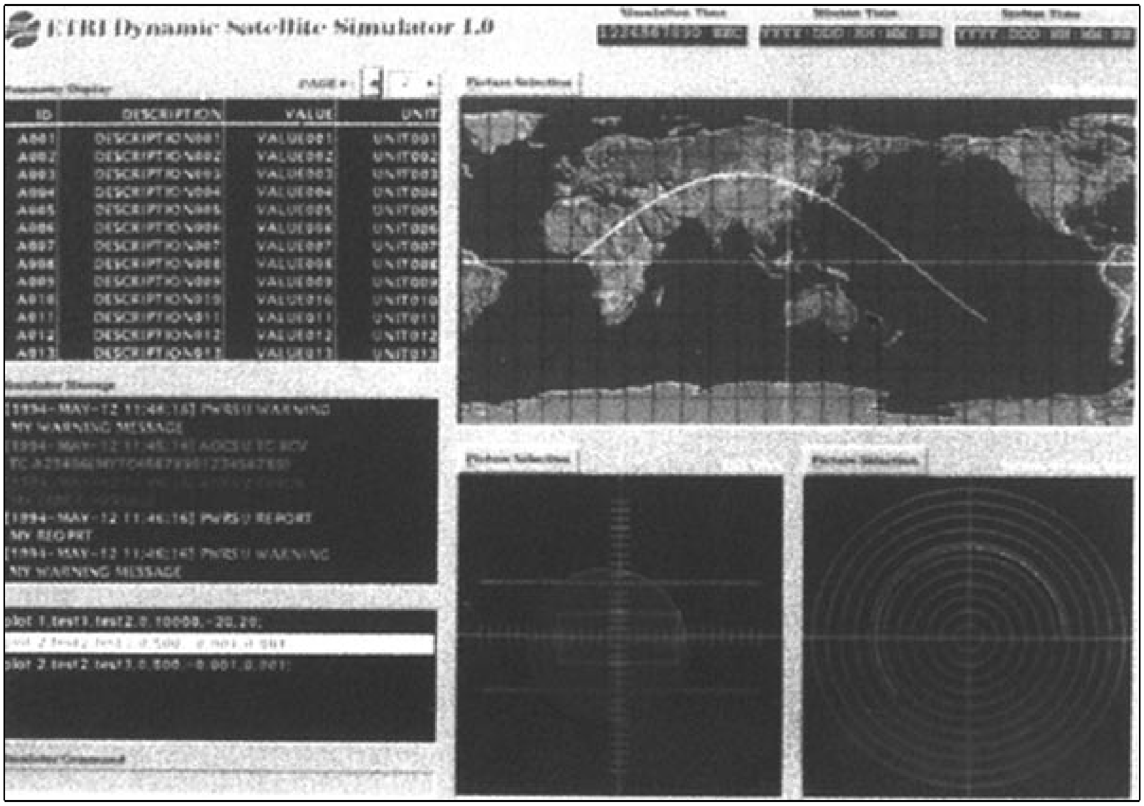

Fig. 6. Operator's console.

lect key variables to be displayed.

C. Log Display

The simulation log keeps track of all significant events taking place during a simulation run.

D. Trend Graphs/Ground Track Display

This window can be used in dual modes allowing the visualization of either simulation variables in graph format or subsatellite trajectories on the earth map, all in real-time. In the graph mode, up to five trend curves can be plotted.

E. Sensor View Window

This window can be used in dual modes. In the preoperational mode, it displays the fields of view of the sun and horizon sensors and the state of satellite attitude with respect to earth, sun and moon. In the operational mode, it displays only the earth sensor field of view and the state of satellite attitude with respect to the earth.

keeping maneuvers.

G. Flight Dynamics Monitors

Two external auxiliary graphic monitors are used to visualize three-dimensional satellite flight states in real-time. The three-dimensional attitude monitor provides a three-dimensional graphic animation of the satellite showing its attitude dynamically as calculated by the attitude dynamics model (Fig. 7). The three-dimensional orbit monitor provides the graphic visualization of the orbital state as calculated by the orbital dynamics model (Fig. 8).

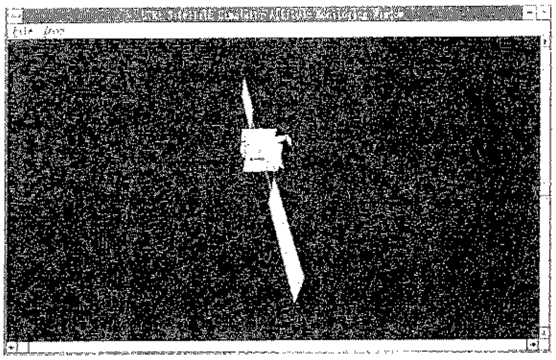

Fig. 7. Three-dimensional attitude graphic monitor.

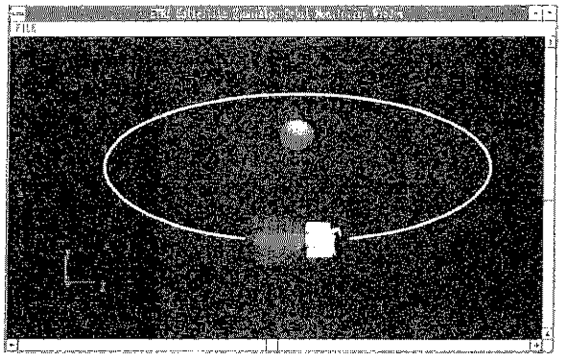

Fig. 8. Three-dimensional orbit graphic monitor.

2. Tracking, Telemetry and Command Interface

This provides an interface between *ARTSS* and the SCC facilities for supporting their ground operations activities such as tracking, telemetering and commanding. All data between *ARTSS* and the SCC pass through the LAN, using DECnet protocol. The LAN connected to the external command source (SCC) is continuously monitored for commands. The communication mechanisms used for the simulator processes are VMS network mailboxes and shared memory.

Telecommand packets from the SCC which specify a command opcode and data word are received by the network mailbox and forwarded to the telecommand handling unit in the simulator kernel block for decoding and distribution.

Telemetry frames generated by the telemetry handling unit in the simulator kernel block are transmitted to the SCC via the LAN every two seconds through the network mailbox. Prior to transmitting the frame, the updating frame counter is inserted. The simulator transmits telemetry only while the simulation is active. On the other hand, if the simulation is paused through the simulator control menu, telemetry transmission will be suspended.

VI. CONCLUSIONS

An advanced real-time satellite simulator, which provides a new satellite simulation environment, has been developed to support the ground operations activities such as control procedures verification, system validation, satellite anomaly analysis and operation team training. The design concept was based on a top-down modular approach. The system was built as a distributed architecture system for easy maintenance. The graphic-enhanced user interface facilities help users have friendly access to the system and easy operation. The real-time graphic monitoring capability, including multi-dimensional visualization of the satellite's attitude and orbit dynamics, provides the operator a sense of virtual reality that he operates an actual in-orbit satellite. Another key feature of *ARTSS* is that the system can simulate most of the functions of a communication satellite system when interfaced with a hardware transponder.

A future goal for the ETRI satellite simulator is to develop the spacecraft model-free simulation tool. Based on such a simulation tool, one can develop a particular satellite simulator efficiently by only modifying or changing the models.

ACKNOWLEDGMENTS

This project has been funded by Korea Telecom and performed as a part of the R&D activities for the satellite operations system related to the Koreasat program.

REFERENCES

[1] Wiley J. Larson and James R. Wertz (editors), *Space Mission Analysis and Design (2nd ed.)*. Torrance, CA: Microcosm, Inc. and Dordrecht/Boston/London: Kluwer Academic Publishers, 1992, pp. 564-568.

[2] A. Ramos, R. L. Minciotti, T. Hampsch, G. Allison, E. W. Hare, and J. W. Opiekun, "Design and Validation of the ITALSAT AOCS Flight Simulator," *COMSAT Technical Review*, vol. 23, no. 1, Spring 1993, pp. 35-60.

[3] James R. Wertz, *Spacecraft Attitude Determination and Control*. Dordrecht, Holland: D. Reidel Publishing Company, 1986, pp. 601-602.

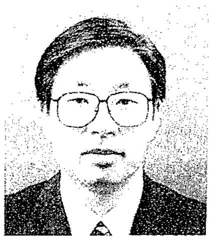

Ja-Young Kang was born in Yeo-ju, Korea in 1954. He received his B. S. degree in mechanical engineering from Chung-Ang University in 1977, M. S. degree from Texas Tech University in 1987, and Ph. D. degree in Aerospace Engineering from Auburn University in 1992. He worked for the Central International Law & Patent Firm from September 1976 to February 1979 and the Agency for Defense Development from March 1979 to August 1984. He was also a part-time instructor in engineering mechanics and mathematics at Kyungnam University during the period from 1980 to 1982. Since he joined the Satellite Communications Division of the ETRI in June 1992, he has worked as the project manager of the Advanced Real-Time Satellite Simulator (ARTSS) development. Dr. Kang is currently in charge of a new satellite simulator development for Korean Multi-Purpose Satellite (KOMPSAT). His recent research is involved with the guidance, control and dynamics of satellite systems. He is a co-author of two engineering books and has published about twenty papers in domestic and international journals and proceedings. Dr. Kang was awarded an honor for the Outstanding Achievement in Academic Excellence by Auburn University in 1991 and is a member of the American Institute of Aeronautics and Astronautics, the Korean Society for Aeronautical and Space Sciences, the Korean Society of Space Technology, and the Korean Society of Mechanical Engineers.

Jae-Moung Kim graduated from Hanyang University with a B. S. degree in electrical engineering in 1974 and MSEE and Ph. D. degrees from University of Southern California in 1982 and Yonsei University in 1987, respectively. He had worked at Korea Institute of Science and Technology (KIST) from 1974 to 1977 and Korea Telecommunications Research Institute (KTRI) from 1977 to 1979. He joined ETRI in 1982, where he is currently working as director of Satellite Communication System Department. His research interests include digital mobile communication and satellite communication systems engineering, especially in the fields of telecommunication system modeling and its performance evaluation.

Seon Jong Chung was born in South Korea in 1943. He received his B. S. degree in electrical engineering from Seoul National University in 1964 and Ph. D. degree in electrical engineering with specialty in communication theory from the Pennsylvania State University in 1976. He worked for Control Data Corp. in St. Paul, USA as a computer system design engineer 4 years. From 1976 to 1983, he worked for Lockheed Electronics, then Ford Aerospace in Johnson Space Center, Houston as an avionics & space communication engineer for the Space Shuttle Project. He returned to Korea in 1983 to join ETRI under the Ministry of Information and Communications. At ETRI, he managed R&D projects for Korea ISDN for six years until 1989. In 1987, he led the national effort in founding Open System Interconnection (OSI) Association of Korea and served as vice president and president until 1992. OSIA later became a member of Asia-Oceania Working Group for OSI and computer network standardization. Since the start of Koreasat project in 1989, he has been vice president for Satellite Communications Division of ETRI. In 1994, Dr. Chung was elected to serve as the president of the Asia-Pacific Satellite Communications Council (APSCC), a regional cooperative body for satellite communications in the Asia-Pacific.